Cytokinins control endocycle onset by promoting the expression of an APC/C activator in *Arabidopsis* roots

Naoki Takahashi[a], Takehiro Kajihara[a], Chieko Okamura[a], Yoonhee Kim[b], Youhei Katagiri[c], Yoko Okushima[a], Sachihiro Matsunaga[c], Ildoo Hwang[b], Masaaki Umeda[a,d,1]

[a]Graduate School of Biological Sciences, Nara Institute of Science and Technology, Takayama 8916-5, Ikoma, Nara 630-0192, Japan; [b]Department of Life Sciences, Pohang University of Science and Technology, Pohang 790-784, Korea; [c]Department of Applied Biological Science, Faculty of Science and Technology, Tokyo University of Science, Yamazaki 2641, Chiba 278-8510, Japan; [d]JST, CREST, Takayama 8916-5, Ikoma, Nara 630-0192, Japan

[1]To whom correspondence should be addressed.

Masaaki Umeda

Graduate School of Biological Sciences

Nara Institute of Science and Technology

Takayama 8916-5, Ikoma, Nara 630-0192, Japan

Tel. +81-743-72-5592 Fax +81-743-72-5599

E-mail: mumeda@bs.naist.jp

Running title: Cytokinins promote endocycle onset in roots

Summary

Plant roots respond to various internal and external signals and adjust themselves to changes of environmental conditions. In the root meristem, stem cells produce daughter cells that continue to divide several times. When these latter cells reach the transition zone, they stop dividing and enter the endocycle, a modified cell cycle in which DNA replication is repeated without mitosis or cytokinesis. The resultant DNA polyploidization, named endoreduplication, is usually associated with an increase of nuclear and cell volume, and with cell differentiation [1-4]. At the transition zone, cytokinin signaling activates two transcription factors, type-B ARABIDOPSIS RESPONSE REGULATOR 1 and 12 (ARR1 and ARR12), and induces *SHY2/IAA3*, a member of the Aux/IAA family of auxin signaling repressors. This inhibits auxin signaling and reduces the expression of auxin efflux carriers, resulting in cell division arrest [5]. Such counteracting actions of two hormones are assumed to determine meristem size. However, it remains unknown whether cytokinins additionally control meristem size through an auxin-independent pathway. Here we show that, in *Arabidopsis*, the cytokinin-activated ARR2 directly upregulates the expression of *CCS52A1*, which encodes an activator of an E3 ubiquitin ligase, anaphase-promoting complex/cyclosome (APC/C) [6], thereby promoting the onset of the endocycle and restricting meristem size. Our genetic data revealed that CCS52A1 function is independent of SHY2-mediated control of auxin signaling, indicating that downregulation of auxin signaling and APC/C-mediated degradation of cell cycle regulators cooperatively promote endocycle onset, and thus fine-tune root growth.

Results and Discussion

Hormonal signaling is likely to control the timing of endocycle onset, but little is known about the molecular mechanisms involved. Because cytokinin is known to restrict meristem size, we first examined whether it affects endocycle onset in the root tip. As reported previously, a 16-h treatment with 1 μM trans-zeatin (tZ) decreased the number of dividing cells in the meristem and thus reduced the meristem size, which corresponds to the number of cortex cells between the quiescent center (QC) and the first elongated cell (Figure 1A and S1A) [7]. Conversely, cell elongation was delayed both in the cytokinin receptor mutant *ahk3-1 ahk4-1*, which is insensitive to exogenous cytokinin application in root elongation [8], and in the cytokinin biosynthesis mutant *ipt3-2 ipt5-1 ipt7-1* [9] (Figure 1A and S1A). Accordingly, root growth was altered as shown in Figure S1B. We then visualized nuclei by DAPI staining, and measured the DNA level (C-value) and cell length for each cell near the transition zone. We found a tight correlation between the two parameters, which was invariable regardless of the integrity of cytokinin signaling (Figure S1C). This indicates that cell elongation in this area depends principally on DNA polyploidization, and that cytokinin controls endocycle onset. To substantiate this result, we examined the correlation between distance from the QC and nuclear area, which is known to correlate well with DNA content [10]. In tZ-treated roots, an increase in nuclear area was noted in cells closer to the QC, whereas in the cytokinin-related mutants the increase occurred in cells further from the QC (Figure 1B and 1C). These results also indicate that cytokinin promotes the transition from the mitotic cell cycle to the endocycle, and consequently increases the DNA level in cells closer to the QC and restricts the meristem size.

Endocycle onset requires a controlled decrease of mitotic cyclin-dependent kinase

(CDK) activities [11]. A major cause of this reduction is the degradation of mitotic cyclins, mediated by an E3 ubiquitin ligase, anaphase-promoting complex/cyclosome (APC/C). APC/C activity is controlled by regulatory proteins, among which activators such as CDH1, Fizzy-related (FZR) and CCS52A are known to promote the onset and progression of the endocycle in human, *Drosophila* and plants, respectively [6, 12, 13]. *Arabidopsis* has two genes for CCS52A, *CCS52A1* and *CCS52A2*, and *CCS52A1* is known to function in mitotic exit and endoreduplication; specifically, CCS52A1 downregulates the B1-type CDK activity by promoting degradation of its partner cyclin A2;3, leading to endocycle onset [6, 14, 15]. As reported previously, a ß-glucuronidase (GUS) reporter line carrying the *CCS52A1* promoter showed GUS expression in the transition and elongation/differentiation zones, but not in the meristematic zone (Figure 1D) [15]. Maximal GUS expression was detected just above the meristematic zone, where endoreduplication starts to occur. In the epidermis, stronger GUS expression was observed in the hair cell layer than in the non-hair cell layer, for unknown reasons (Figure 1D and 1E, wild-type). Nuclear-localized GFP expressed under the *CCS52A1* promoter started to accumulate in a few cells preceding the first endoreduplicated cell (Figure S1D and S1E), supporting the idea that CCS52A1 is involved in endocycle onset.

Since cytokinins appear to promote endoreduplication, as described above, we hypothesized that cytokinin signaling regulates *CCS52A1* expression. To test this, we monitored *CCS52A1* promoter activity under different cytokinin conditions. tZ treatment for 3 h elevated *ProCCS52A1:GUS* expression in the transition and elongation/differentiation zones, but not in the meristematic zone (Figure 1D). This indicates that the spatial expression pattern of *CCS52A1* is not dependent on cytokinin

distribution in roots; rather, cytokinins modulate the transcript level. qRT-PCR also showed cytokinin-induced upregulation of *CCS52A1* expression (Figure S1F). In the cytokinin receptor mutants, *CCS52A1* expression was reduced and restricted almost entirely to the transition zone (Figure 1E and S1F). Furthermore, overexpression of the *cytokinin oxidase 2* (*CKX2*) gene, which lowers the endogenous cytokinin level by degrading active forms of cytokinins [16], also resulted in a reduction of *ProCCS52A1:GUS* expression (Figure 1E). These results indicate that *CCS52A1* expression is under the control of cytokinin signaling.

Plant cells respond to cytokinins through a two-component phosphorelay pathway, in which the phosphate group is transferred to the type-B ARABIDOPSIS RESPONSE REGULATOR (ARR) transcription factors. Phosphorylated type-B ARRs control transcription of cytokinin response genes [17]. To determine which part of the *CCS52A1* promoter is necessary for cytokinin response, we made a deletion series from the 5' end and observed the promoter activity by generating GUS-fusion genes. The results showed that deletion of the sequence between -990 bp and -890 bp from the start codon almost abolished the promoter activity (Figure S2A and S2B). This region contains one consensus ARR-binding sequence (5'-GATT-3') [18] at -932 bp from the start codon.

To test whether type-B ARRs can physically associate with the *CCS52A1* promoter, we performed a yeast one-hybrid assay with two type-B ARRs, ARR1 and ARR2. Generally, the N-terminal region of type-B ARRs contains three separated amino acids (two aspartates and a lysine; the DDK domain) whose aspartates receive

the phosphate group. Upon phosphorylation of the DDK domain, the N-terminal region loses its repressive function in transcriptional activation; thus, artificial removal of the N-terminal region generates a constitutive active ARR [18]. As shown in Figure 2A, ARR2 lacking the DDK domain (ARR2ΔDDK) associated with the 1.5-kb promoter region of *CCS52A1*, but no interaction was observed with full-length ARR2, or with ARR1 regardless of the DDK domain. We further examined *in vivo* targets of ARR2 by chromatin immunoprecipitation (ChIP) using *Arabidopsis* plants expressing hemagglutinin (HA)-tagged ARR2. Immunoprecipitation with anti-HA antibody, followed by PCR with specific primer sets, revealed that the highest enrichment of ARR2-bound chromatin was for the promoter region between -1000 bp and -800 bp from the start codon (Figure 2B and 2C). This region corresponds to that required for GUS expression in the promoter deletion analysis (Figure S2A and S2B). These data demonstrate that *CCS52A1* is a direct target of the active form of ARR2.

A transient activation assay using *Arabidopsis* protoplasts showed that the *CCS52A1* promoter activity was induced by overexpression of ARR2ΔDDK, and slightly increased by expression of full-length ARR2 (Figure 2D). The promoter activity in protoplasts transfected with full-length ARR2 was elevated by tZ application and reached the level of ARR2ΔDDK overexpression (Figure S2C), suggesting low cytokinin content in protoplasts. In contrast, no significant change was observed when the other type-B ARRs, ARR1, ARR10 and ARR12, with or without the DDK domain, were overexpressed (Figure 2D). In planta, *CCS52A1* expression, which was monitored with the *ProCCS52A1:GUS* reporter gene and qRT-PCR, decreased in roots of the

ARR2 knockout mutant *arr2-4* (Figure 2E and S1F). However, its promoter activity was not altered in the *ARR1* or *ARR12* knockout mutants (Figure S2D and S2E). These results demonstrate that ARR2, but not ARR1 or the other type-B ARRs, induces *CCS52A1* expression. ARR2-GUS fusion protein expressed under the *ARR2* promoter started to accumulate in a few cells preceding the first elongated cell, as observed for the *CCS52A1* promoter activity (Figure 2F and 2G) [19], supporting the role of ARR2 in inducing *CCS52A1* expression.

To determine whether ARR2-mediated induction of *CCS52A1* plays a physiological role in the transition to the endocycle, we first measured root meristem size of *ccs52a1* and *arr2* mutants. As previously reported, the knockout mutant *ccs52a1-1* had more cells in the meristematic zone than wild-type (Figure 3) [15]. Root meristem size was reduced by tZ treatment in wild-type, but less so in *ccs52a1-1*. *arr2-4* and the other *arr2* knockout mutants, *arr2-3* and *arr2-5*, also had a larger meristem and showed lower sensitivity to tZ than wild-type (Figure 3 and S3A). Furthermore, the root meristem phenotype of the *ccs52a1-1 arr2-4* double mutant was nearly identical to that of *ccs52a1-1* or *arr2-4* single mutants (Figure 3B), suggesting that *CCS52A1* and *ARR2* function in the same pathway. By contrast, transgenic plants overexpressing *ARR2* or *CCS52A1* [6, 20] showed a significant reduction of meristematic cell number, and the sensitivity to tZ was higher in *ARR2*-overexpressing plants than in wild-type (Figure 3B). Similar trends were also observed when we measured root length and the distance between the QC and the first cell harboring an enlarged nucleus (as estimated by an increase of > 1.5-fold in nuclear area) (Figure S3B

and S3C). In *arr2-4*, *ccs52a1-1* and *arr2-4 ccs52a1-1*, root growth in the absence of tZ was almost the same as that in wild-type (Figure S3C), suggesting that ARR2 and CCS52A1 have another role in cell growth in the elongation/differentiation zone. These results indicate that cytokinin-triggered induction of endocycle onset and the resultant reduction in meristem size are associated with ARR2-mediated induction of *CCS52A1*.

A previous report showed that, in the transition zone, ARR1 and ARR12 induce the expression of *SHY2*, and repress auxin signaling and *PIN-FORMED1* (*PIN1*) expression, resulting in cell division arrest [5]. Although ARR1 and ARR12 are not associated with *CCS52A1* expression, as described above, the possibility remained that *CCS52A1* affects auxin signaling and inhibits cell division. To address this point, we applied indole-3-acetic acid (IAA) and the auxin antagonist PEO-IAA [21] to the *ccs52a1* mutant. The root meristem size of *ccs52a1-1* was increased by IAA treatment and reduced by PEO-IAA treatment in a similar fashion to that of wild-type roots (Figure S3D and S3E). Moreover, exogenous IAA treatment did not affect the expression level of *CCS52A1* in wild-type roots (Figure S3F). These results suggest that CCS52A1 functions independently of the auxin-mediated regulation of meristem size.

We next examined the relationship between the ARR2–CCS52A1 and ARR1/12–SHY2 pathways. As mentioned above, the number of meristematic cells was elevated in *ccs52a1-1*, and we found that the *arr1-3 arr12-1* double mutant showed a similar degree of meristem enlargement (Figure 4A and 4B) [5]. However, the *arr1-2 arr12-1 ccs52a1-1* triple mutant displayed a much larger meristem (Figure 4A and 4B). Similarly, *shy2-31 ccs52a1-1* double mutants exhibited a larger meristem than either

shy2-31 or *ccs52a1-1* (Figure S4A and S4B). tZ treatment reduced the meristem size in wild-type and had a milder effect in *ccs52a1-1* or *arr1-3 arr12-1*, but the *arr1-2 arr12-1 ccs52a1-1* triple mutant was completely insensitive to tZ (Figure 4A and 4B). We again observed similar trends when root length and the distance between the QC and the first cell harboring an enlarged nucleus were measured (Figure S3B, S4C and S4D). These data demonstrate that both ARR2–CCS52A1 and ARR1/12–SHY2 pathways are crucial for the control of endocycle onset and root meristem size through cytokinin signaling.

We noticed that, in the presence of tZ, *ARR2* overexpression reduced meristem size more severely than *CCS52A1* overexpression (Figure 3B and S3B). Moreover, *ARR2* overexpression in *ccs52a1-1* reduced the meristem size, relative to that in *ccs52a1-1*, and this effect was enhanced by tZ treatment (Figure 3B and S3B). These results indicate that ARR2 regulates not only *CCS52A1* but also other factors involved in the control of endocycle onset and meristem size. One possibility is that ARR2, like ARR1 and ARR12, suppresses auxin signaling by controlling *SHY2* expression. Our measurement of the *SHY2* transcript level showed that *SHY2* expression decreased in *arr2-4* as observed in *arr1-3*, *arr12-1*, and *arr1-3 arr12-1* (Figure S4E). This indicates that ARR2 regulates not only *CCS52A1* but also *SHY2* expression and controls auxin signaling. However, as mentioned above, the extent of meristem enlargement observed in *arr2-4* was almost the same as that in *ccs52a1-1*, and *arr2-4* was not fully resistant to tZ (Figure 3B). Therefore, while ARR2-mediated control of *CCS52A1* contributes substantially to endocycle onset, a group of type-B ARRs (ARR1, ARR2, ARR12)

cooperate in the upregulation of *SHY2* expression and suppression of auxin signaling.

In summary, this study has shown that cytokinin controls endocycle onset and meristem size through an auxin-independent pathway; namely, cytokinin-activated ARR2 directly induces the expression of *CCS52A1*, which activates the E3 ubiquitin ligase APC/C and promotes the degradation of mitotic regulators, causing cell division to cease (Figure 4C). This pathway is distinct from the ARR1/12–SHY2 pathway, in which cytokinin counteracts auxin and inhibits cell division (Figure 4C) [5]. It is likely that the ARR2–CCS52A1 pathway acts in the precise control of endocycle onset by promoting the degradation of cell cycle regulators in the transition zone, thereby fine-tuning meristem size. In this study, we also found that ARR2 regulates not only *CCS52A1* but also *SHY2* expression (Figure 4C). Choi et al. [20] reported that ARR2 functions in the defense response with another transcription factor, TGA3, via a direct interaction. Therefore, in the transition zone of roots, ARR2 may have a specific interaction partner to bind to the *CCS52A1* promoter but not to the *SHY2* promoter which is recognized also by ARR1 and ARR12 [5]. A recent report showed that the ubiquitin-proteasome pathway brings about immediate degradation of the ARR2 protein [19], suggesting that ARR2-mediated control of the cell cycle is strictly regulated at multiple levels. Further studies on ARR2 target genes will reveal how cytokinins control the phase change from the mitotic cell cycle to the endocycle and how they contribute to cell growth and differentiation in roots.

Supplemental Information

Supplemental Information includes four figures, one table and Supplemental Experimental Procedures, and can be found with this article online.

Acknowledgements

We thank Eva Kondorosi, Tatsuo Kakimoto, Chiharu Ueguchi, Thomas Schmülling, and the Arabidopsis Biological Research Center for providing mutants and transgenic plants. We also thank Kenichiro Hayashi for providing PEO-IAA. This work was supported by MEXT KAKENHI Grant Number 22119009, and by JST, CREST.

References

1. Perilli, S., Di Mambro, R., and Sabatini, S. (2012). Growth and development of the root apical meristem. Curr. Opin. Plant Biol. *15*, 17-23.
2. Melaragno, J.E., Mehrotra, B., and Coleman, A.W. (1993). Relationship between endopolyploidy and cell size in epidermal tissue of Arabidopsis. Plant Cell *5*, 1661-1668.
3. Traas, J., Hülskamp, M., Gendreau, E., and Höfte, H. (1998). Endoreduplication and development: rule without dividing? Curr. Opin. Plant. Biol. *1*, 498-503.
4. Sugimoto-Shirasu, K., and Roberts, K. (2003). "Big it up": endoreduplication and cell-size control in plants. Curr. Opin. Plant Biol. *6*, 544-553.
5. Dello Ioio, R., Nakamura, K., Moubayidin, L., Perilli, S., Taniguchi, M., Morita, M.T., Aoyama, T., Costantino, P., and Sabatini, S. (2008). A genetic framework for the control of cell division and differentiation in the root meristem. Science *322*, 1380-1384.
6. Larson-Rabin, Z., Li, Z., Masson, P.H., and Day, C.D. (2009). *FZR2/CCS52A1* expression is a determinant of endoreduplication and cell expansion in Arabidopsis. Plant Physiol. *149*, 874-884.
7. Dello Ioio, R., Linhares, F.S., Scacchi, E., Casamitjana-Martinez, E., Heidstra, R., Costantino, P., and Sabatini, S. (2007). Cytokinins determine *Arabidopsis* root-meristem size by controlling cell differentiation. Curr. Biol. *17*, 678-682.
8. Higuchi, M., Pischke, M.S., Mähönen, A.P., Miyawaki, K., Hashimoto, Y., Seki, M., Kobayashi, M., Shinozaki, K., Kato, T., Tabata, S., et al. (2004). *In planta* functions

of the *Arabidopsis* cytokinin receptor family. Proc. Natl. Acad. Sci. USA *101*, 8821-8826.

9. Miyawaki, K., Tarkowski, P., Matsumoto-Kitano, M., Kato, T., Sato, S., Tarkowska, D., Tabata, S., Sandberg, G., and Kakimoto, T. (2006). Roles of Arabidopsis ATP/ADP isopentenyltransferases and tRNA isopentenyltransferases in cytokinin biosynthesis. Proc. Natl. Acad. Sci. USA *103*, 16598-16603.
10. Ishida, T., Adachi, S., Yoshimura, M., Shimizu, K., Umeda, M., and Sugimoto, K. (2010). Auxin modulates the transition from the mitotic cycle to the endocycle in *Arabidopsis*. Development *137*, 63-71.
11. Edgar, B.A., and Orr-Weaver, T.L. (2001). Endoreplication cell cycles: more for less. Cell *105*, 297-306.
12. Lasorella, A., Stegmüller, J., Guardavaccaro, D., Liu, G., Carro, M.S., Rothschild, G., de la Torre-Ubieta, L., Pagano, M., Bonni, A., and Iavarone, A. (2006). Degradation of Id2 by the anaphase-promoting complex couples cell cycle exit and axonal growth. Nature *442*, 471-474.
13. Zielke, N., Querings, S., Rottig, C., Lehner, C., and Sprenger, F. (2008). The anaphase-promoting complex/cyclosome (APC/C) is required for rereplication control in endoreplication cycles. Genes Dev. *22*, 1690-1703.
14. Boudolf, V., Lammens, T., Boruc, J., Van Leene, J., Van Den Daele, H., Maes, S., Van Isterdael, G., Russinova, E., Kondorosi, E., Witters, E., et al. (2009). CDKB1;1 forms a functional complex with CYCA2;3 to suppress endocycle onset. Plant Physiol. *150*, 1482-1493.

15. Vanstraelen, M., Baloban, M., Da Ines, O., Cultrone, A., Lammens, T., Boudolf, V., Brown, S.C., De Veylder, L., Mergaert, P., and Kondorosi, E. (2009). APC/C^{CCS52A} complexes control meristem maintenance in the *Arabidopsis* root. Proc. Natl. Acad. Sci. USA *106*, 11806-11811.

16. Werner, T., Motyka, V., Laucou, V., Smets, R., Van Onckelen, H., and Schmülling, T. (2003). Cytokinin-deficient transgenic Arabidopsis plants show multiple developmental alterations indicating opposite functions of cytokinins in the regulation of shoot and root meristem activity. Plant Cell *15*, 2532-2550.

17. Hwang, I., Sheen, J., and Müller, B. (2012). Cytokinin signaling networks. Annu. Rev. Plant Biol. *63*, 353-380.

18. Sakai, H., Aoyama, T., and Oka, A. (2000). *Arabidopsis* ARR1 and ARR2 response regulators operate as transcriptional activators. Plant J. *24*, 703-711.

19. Kim, K., Ryu, H., Cho, Y.H., Scacchi, E., Sabatini, S., and Hwang, I. (2012). Cytokinin-facilitated proteolysis of ARABIDOPSIS RESPONSE REGULATOR 2 attenuates signaling output in two-component circuitry. Plant J. *69*, 934-945.

20. Choi, J., Huh, S.U., Kojima, M., Sakakibara, H., Paek, K.H., and Hwang, I. (2010). The cytokinin-activated transcription factor ARR2 promotes plant immunity via TGA3/NPR1-dependent salicylic acid signaling in *Arabidopsis*. Dev. Cell *19*, 284-295.

21. Hayashi, K., Hatate, T., Kepinski, S., and Nozaki, H. (2008). Design and synthesis of auxin probes specific to TIR1, auxin receptor. Regul. Plant Growth Dev. Suppl. *43*, 95.

Figure Legends

Figure 1. Cytokinins promote endocycle onset and upregulate *CCS52A1* expression in roots.

(A) Root meristem of 5-day-old wild-type, wild-type treated with 1 μM tZ for 16 h, *ahk3-1 ahk4-1*, and *ipt3-2 ipt5-1 ipt7-1* plants. Arrowheads indicate the QC and the first elongated cell in the cortex cell file (insets show enlargements of the boundary region). Bar = 100 μm.

(B) Fluorescence microscopy images of DAPI-stained nuclei of roots. Five-day-old wild-type, wild-type treated with 1 μM tZ for 16 h, *ahk3-1 ahk4-1*, and *ipt3-2 ipt5-1 ipt7-1* plants were observed. Arrowheads indicate the position of the first elongated hair cell in the epidermis. Bar = 100 μm.

(C) Nuclear area and distance from the QC for individual epidermal cells. Six consecutive hair cells surrounding the first elongated cell, indicated by boxes in (B), were quantified. Data were collected from four different samples. Dotted lines mark the average distance from the QC to the first elongated cell ($n \geq 8$), with numerical values shown at the top of each graph.

(D and E) GUS staining of roots of 5-day-old seedlings harboring the *ProCCS52A1:GUS* reporter gene. Wild-type, wild-type treated with 1 μM tZ for 3 h (D), *ahk3-1*, *ahk4-1*, and *35S:CKX2* plants (E). Arrowheads indicate the QC and the first elongated cell in the cortex cell file. Bar = 100 μm.

Figure 2. ARR2 directly induces *CCS52A1* expression.

(A) Yeast one-hybrid assay with the *CCS52A1* promoter. Yeast cells carrying the reporter construct were transformed with the coding regions of *ARR1*, *ARR1ΔDDK*, *ARR2* and *ARR2ΔDDK* fused to the GAL4 activation domain, and yeast cultures were diluted and spotted on plates with (+His) or without (-His) histidine in the presence of 5 mM 3-aminotriazole. The empty vector was used as a control.

(B) Schematic representation of the *CCS52A1* promoter. Thick and thin lines depict the coding and non-coding regions, respectively. The arrow indicates the transcription start site, and the numbers represent position (bp) from the start codon. Black bars shown below illustrate DNA fragments amplified by ChIP-PCR.

(C) ChIP assay. Chromatin bound to ARR2 was collected by immunoprecipitation with anti-HA antibodies from *35S:ARR2-HA* plants. Fold enrichment for each DNA fragment was determined by normalizing the recovery rate against that of wild-type plants. The numbers for each DNA fragment correspond to those in (B).

(D) Protoplast transactivation assay with the *ProCCS52A1:fLUC* reporter gene. Luciferase activity was normalized to *35S:rLUC* and is indicated as relative values, with that for the effector control (*35S:GFP*) set to 1. Data are presented as mean ± SD (n = 3). Significant differences from the control were determined by Student's *t*-test: *, $P < 0.05$; **, $P < 0.01$; the other differences are not significant ($P > 0.05$).

(E) GUS staining of roots of 5-day-old wild-type and *arr2-4* plants harboring *ProCCS52A1:GUS*. Bar = 100 μm.

(F and G) GUS staining of 5-day-old roots harboring *ProARR2:ARR2-GUS*. A

magnified image of the boundary region, indicated by the box in (F), is shown in (G). Bars = 100 μm (F) and 25 μm (G).

Figure 3. ARR2 and CCS52A1 are involved in cytokinin-induced endocycle onset.

(A) Root meristem of 5-day-old wild-type, *ccs52a1-1* and *arr2-4* seedlings. Plants were treated with or without 1 μM tZ for 16 h. Arrowheads indicate the QC and the first elongated cell in the cortex cell file (insets show enlargements of the boundary region). Bar = 100 μm.

(B) Cortex cell number in the meristematic zone. Five-day-old seedlings were treated with or without 1 μM tZ for 16 h, and cell number was counted. Data are presented as mean ± SD (n > 30). Significant differences from the non-treated control were determined by Student's *t*-test: **, $P < 0.01$; ***, $P < 0.001$.

Figure 4. Genetic interaction between *CCS52A1* and *ARR1/12*.

(A) Root meristem of 5-day-old wild-type, *ccs52a1-1*, *arr1-3 arr12-1*, and *arr1-3 arr12-1 ccs52a1-1* seedlings. Plants were treated with or without 1 μM tZ for 16 h. Arrowheads indicate the QC and the first elongated cell in the cortex cell file (insets show enlargements of the boundary region). Bar = 100 μm.

(B) Cortex cell numbers in the meristematic zones shown in (A). Data are presented as mean ± SD (n > 35). Significant differences from the non-treated control were determined by Student's *t*-test: **, $P < 0.01$; ***, $P < 0.001$; the other difference is not significant ($P > 0.05$).

(C) Model for cytokinin-mediated regulation of root meristem size. Cytokinin-activated ARR1 and ARR12 induce *SHY2* expression, leading to a downregulation of *PIN* expression and auxin signaling. Auxin promotes degradation of SHY2. On the other hand, activated ARR2 directly induces *CCS52A1* expression, resulting in the degradation of cell cycle regulators and promoting the transition from the mitotic cell cycle to the endocycle. Both pathways are crucial for the control of endocycle onset and root meristem size. ARR2 also induces *SHY2* expression. AHKs, Arabidopsis histidine kinases.

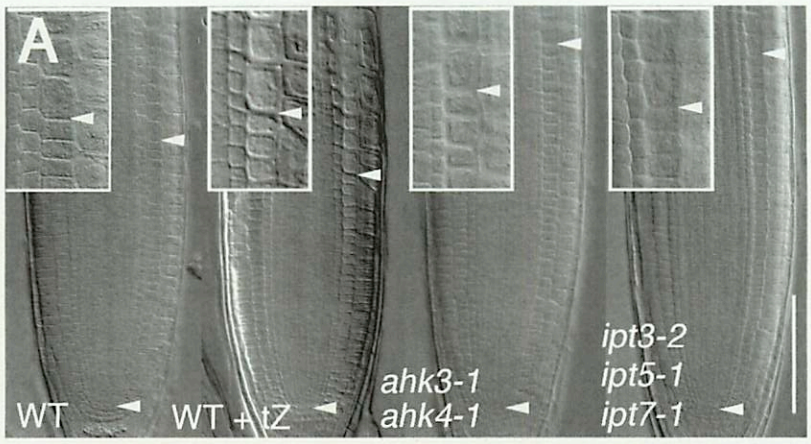
A
WT
WT + tZ
ahk3-1
ahk4-1
ipt3-2
ipt5-1
ipt7-1

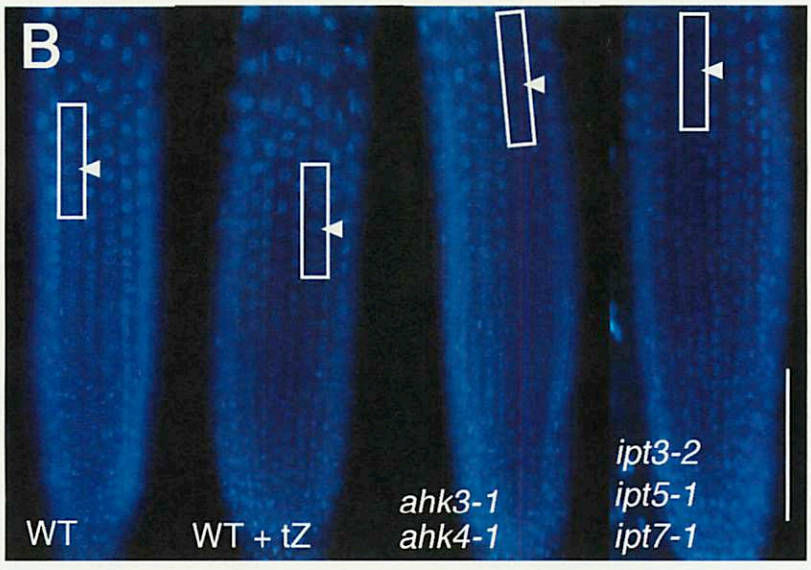
B
WT
WT + tZ
ahk3-1
ahk4-1
ipt3-2
ipt5-1
ipt7-1

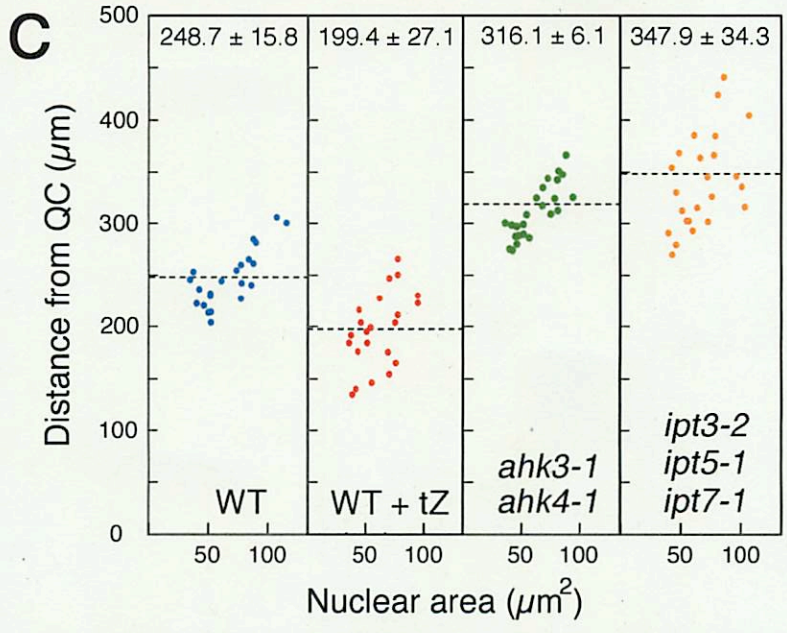
C
248.7 ± 15.8
199.4 ± 27.1
316.1 ± 6.1
347.9 ± 34.3
Distance from QC (μm)
500
400
300
200
100
0
WT
WT + tZ
ahk3-1
ahk4-1
ipt3-2
ipt5-1
ipt7-1
50
100
Nuclear area (μm²)

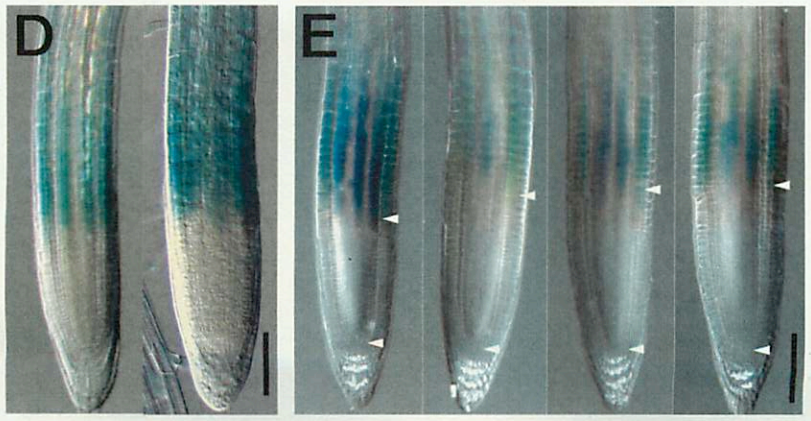
D
E
WT
WT + tZ
WT
ahk3-1
ahk4-1 35S:CKX2

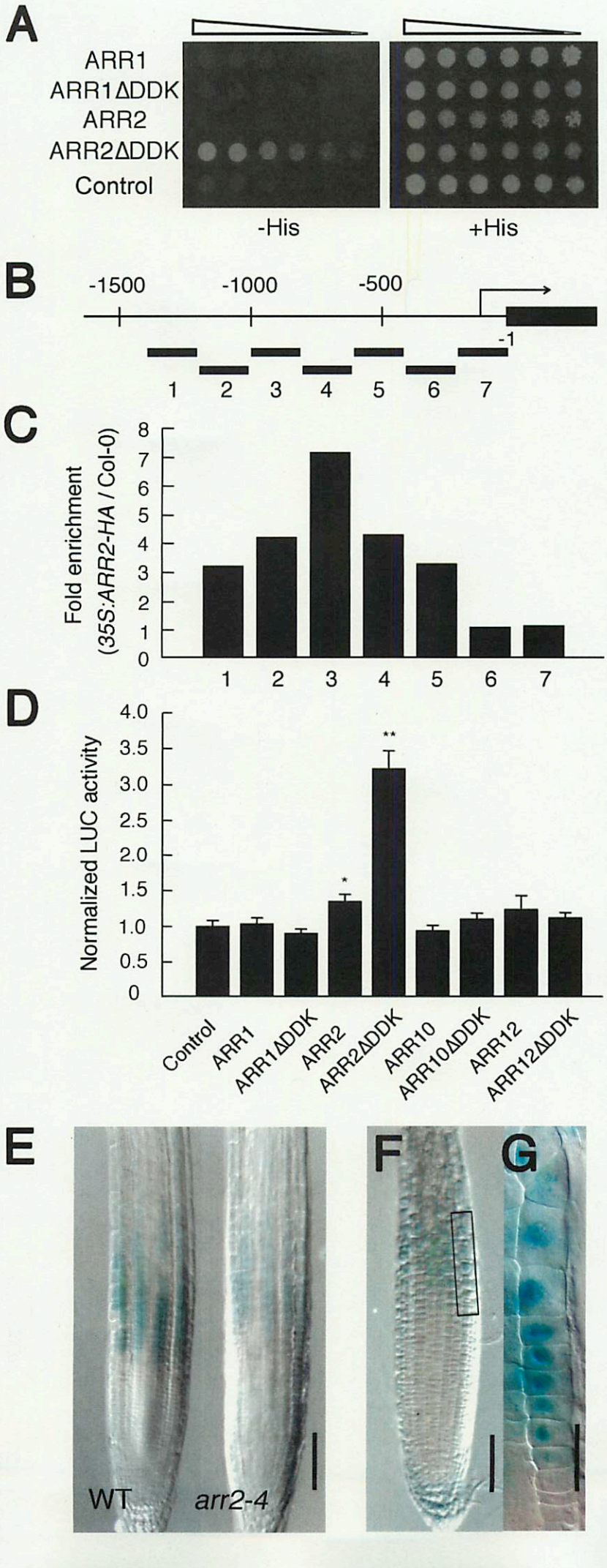
A
ARR1
ARR1ΔDDK
ARR2
ARR2ΔDDK
Control
-His
+His
B
-1500
-1000
-500
-1
1
2
3
4
5
6
7
C
Fold enrichment
(35S:ARR2-HA / Col-0)
0
1
2
3
4
5
6
7
8
1
2
3
4
5
6
7
D
Normalized LUC activity
0
0.5
1.0
1.5
2.0
2.5
3.0
3.5
4.0
*
**
Control
ARR1
ARR1ΔDDK
ARR2
ARR2ΔDDK
ARR10
ARR10ΔDDK
ARR12
ARR12ΔDDK
E
WT
arr2-4
F
G

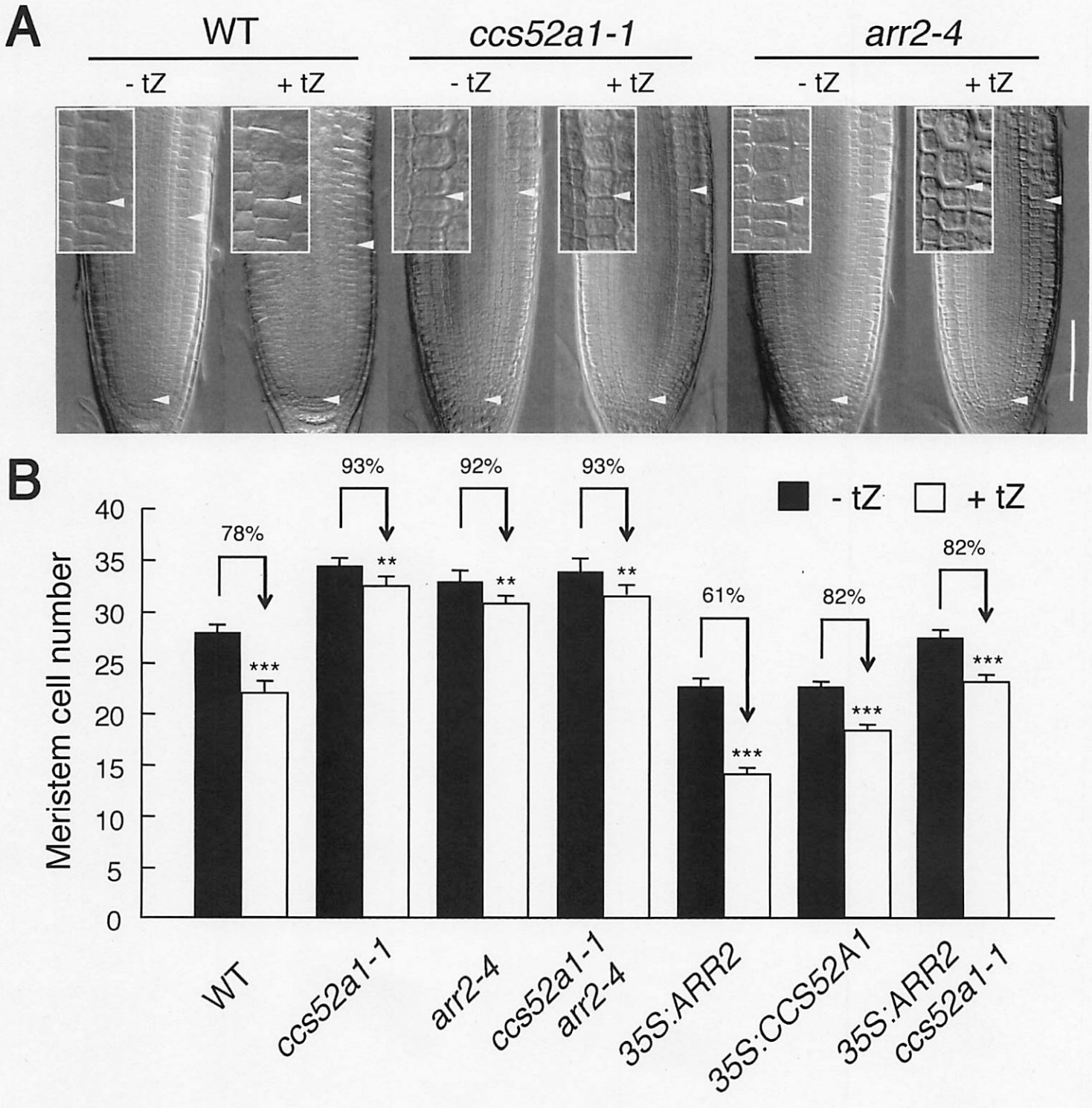
A
WT
ccs52a1-1
arr2-4
- tZ
+ tZ
- tZ
+ tZ
- tZ
+ tZ
B
- tZ
+ tZ
Meristem cell number
0
5
10
15
20
25
30
35
40
78%
93%
92%
93%
61%
82%
82%
***
**
**
**
***
***
***
WT
ccs52a1-1
arr2-4
ccs52a1-1 arr2-4
35S:ARR2
35S:CCS52A1
35S:ARR2 ccs52a1-1

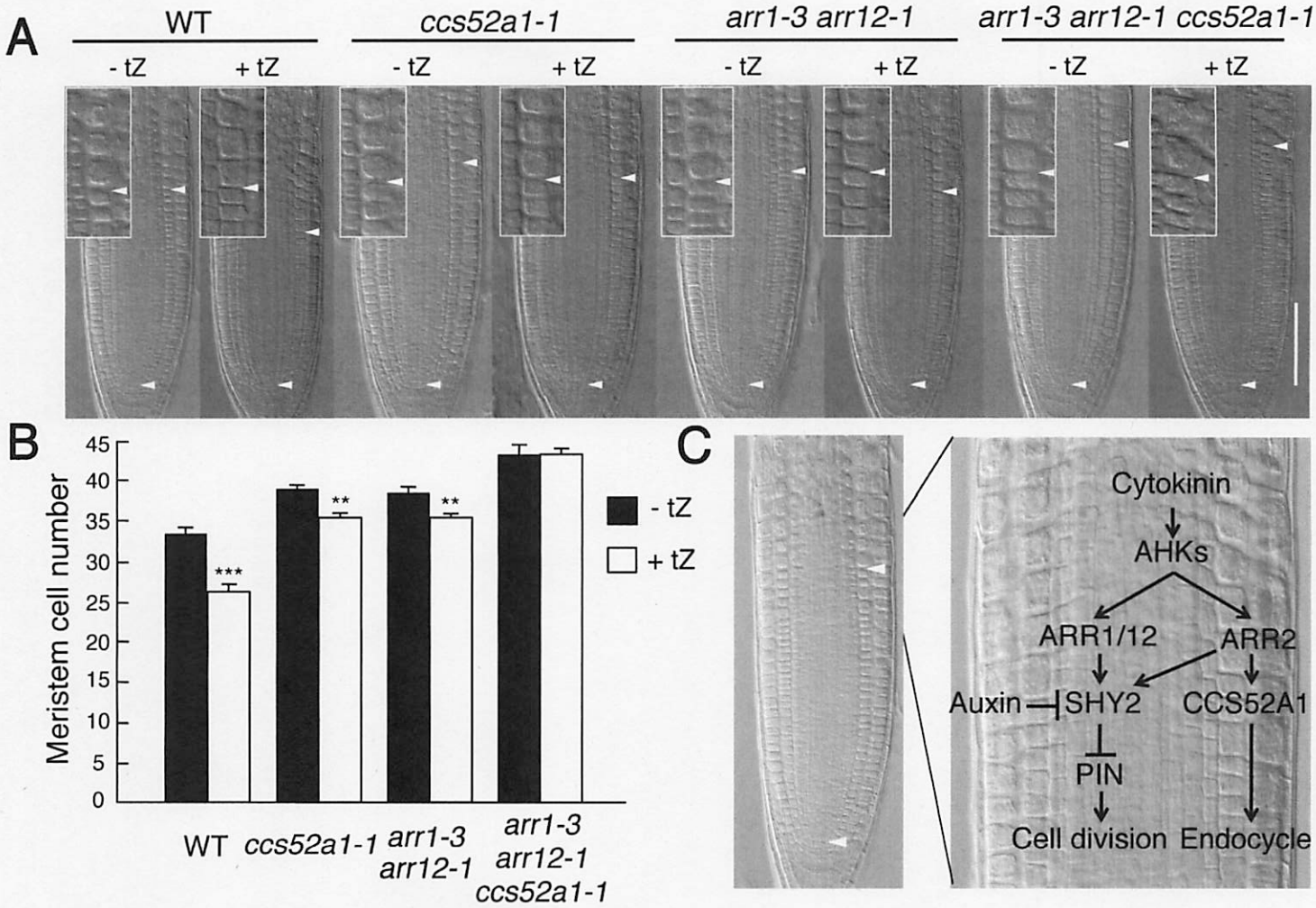
A
WT
ccs52a1-1
arr1-3 arr12-1
arr1-3 arr12-1 ccs52a1-1
- tZ
+ tZ
B
Meristem cell number
45
40
35
30
25
20
15
10
5
0
***
**
**
- tZ
+ tZ
WT
ccs52a1-1
arr1-3 arr12-1
arr1-3 arr12-1 ccs52a1-1
C
Cytokinin
AHKs
ARR1/12
ARR2
Auxin
SHY2
CCS52A1
PIN
Cell division
Endocycle

SUPPLEMENTAL INFORMATION

Cytokinins control endocycle onset by promoting the expression of an APC/C activator in *Arabidopsis* roots

Naoki Takahashi, Takehiro Kajihara, Chieko Okamura, Yoonhee Kim, Youhei Katagiri, Yoko Okushima, Sachihiro Matsunaga, Ildoo Hwang, and Masaaki Umeda

Inventory of Supplemental Information

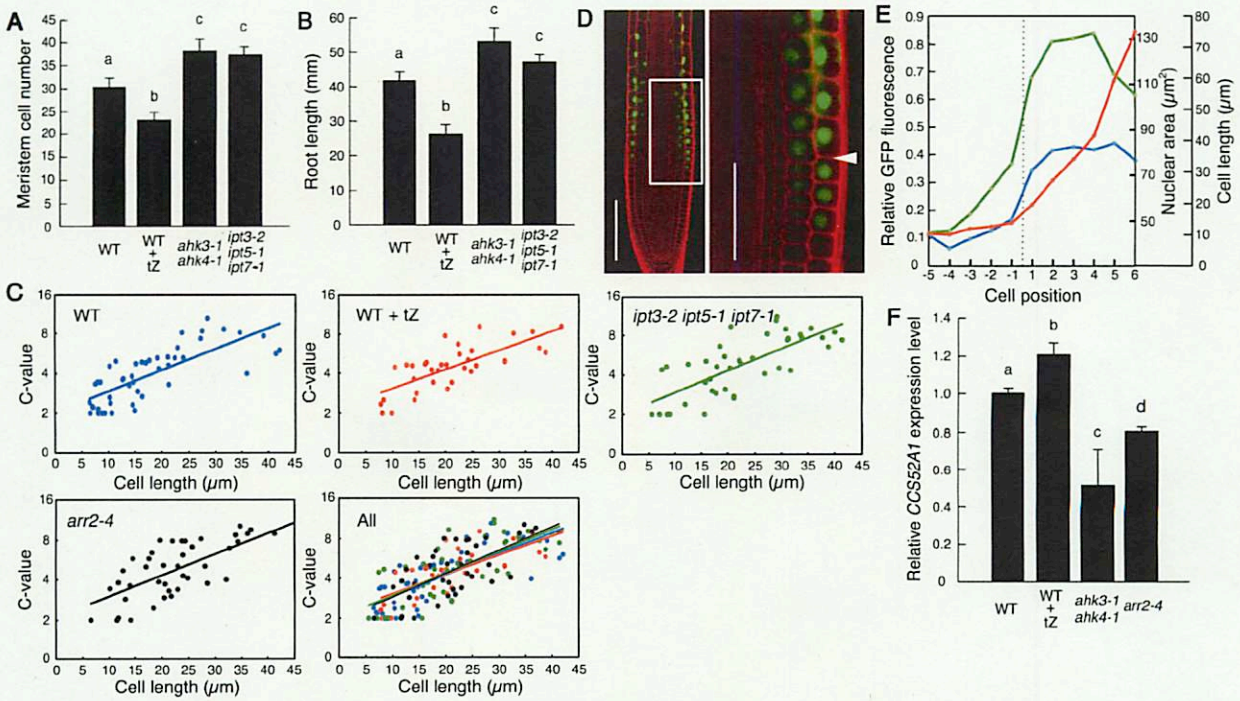

Figure S1 (Related to Figure 1). Cytokinins reduce meristem size and upregulate *CCS52A1* expression in *Arabidopsis* roots.

(A) Cortex cell number in the meristematic zone. Cortex cells flanked by the two arrowheads in Figure 1A were counted. Bars with different letters differ significantly from each other ($P < 0.05$).

(B) Root length of 10-day-old wild-type, wild-type grown on medium containing 100 nM tZ, *ahk3-1 ahk4-1*, and *ipt3-2 ipt5-1 ipt7-1* plants. Data are presented as mean ± SD (n > 25). Bars with different letters differ significantly from each other ($P < 0.05$).

(C) Correlation between cell length and DNA ploidy. Cell length and C-value of cells near the transition zone were measured and quantified in 5-day-old wild-type, wild-type treated with 1 μM tZ for 16 h, *ipt3-2 ipt5-1 ipt7-1*, and *arr2-4* plants (n ≥ 4). Fluorescence intensity of DAPI-stained nuclei was quantified and is displayed as C-value. 'All' shows the combined data of the four plants. Regression lines are included; $R^2 = 0.57$ (WT), 0.56 (WT + tZ), 0.54 (*ipt3-2 ipt5-1 ipt7-1*), and 0.50 (*arr2-4*); $F < 0.001$ for all regression analysis.

(D) Confocal microscopy images of 5-day-old roots harboring the *ProCCS52A1:NLS-GFP* reporter gene. The boundary region between the meristematic zone and the transition zone is indicated by the box, and is magnified in the right image. The arrowhead indicates the boundary between the last mitotic cell and the first endoreduplicated cell in the epidermis, which was estimated by an increase of > 1.5-fold in nuclear area. Bars = 100 μm (left) and 50 μm (right).

(E) *CCS52A1* expression, nuclear area and cell length in the region surrounding the first endoreduplicated cell. Transgenic roots shown in (D) were used to measure GFP fluorescence (green), nuclear area (blue) and cell length (red), and average values are quantified (n=18). The dotted line corresponds to the position of the boundary between the meristematic region and the first endoreduplicated cell, which is indicated by an arrowhead in (D). Cell position '1' indicates the first endoreduplicated cell, which is preceded by the last mitotic cell before

entry into the endocycle (cell position '-1').
(F) *CCS52A1* mRNA level in root tips. Total RNA from 5-day-old roots was subjected to real-time qRT-PCR. For cytokinin application, seedlings were treated with 1 μM tZ for 1 h. The expression levels of *CCS52A1* were normalized to that of *ACTIN2*, and are indicated as relative values, with that for wild-type set to 1. Data are presented as mean ± SD (n = 3). Bars with different letters differ significantly from each other ($P < 0.05$).

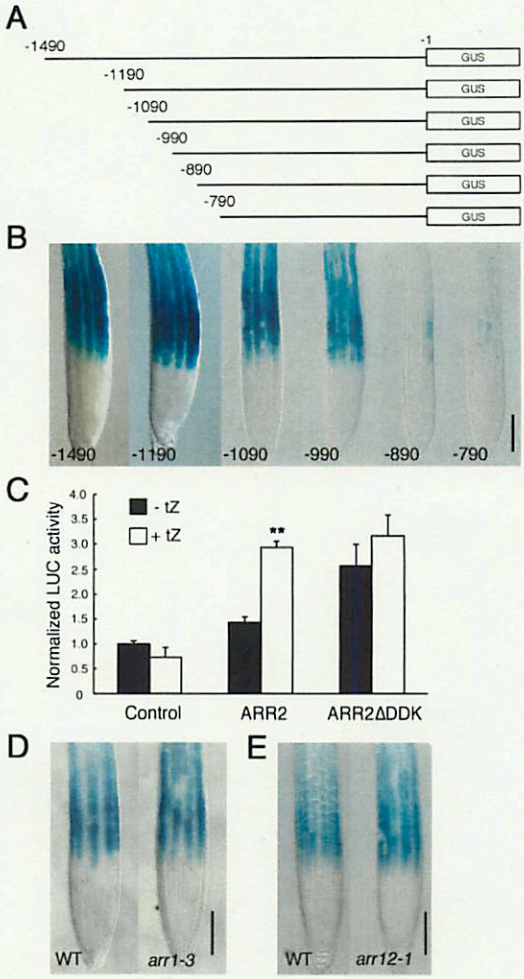

Figure S2 (Related to Figure 2). *CCS52A1* promoter activity in roots.

(A) GUS reporter constructs carrying intact (top line) and progressively truncated *CCS52A1* promoter fragments. Numbers indicate the distance (bp) from the start codon.

(B) GUS staining of roots of 5-day-old seedlings harboring each construct listed in (A). Bar = 100 μm.

(C) Cytokinin-activated ARR2 induces *CCS52A1* expression. A protoplast transactivation assay was conducted with the *ProCCS52A1:fLUC* reporter gene. Transfected protoplasts were treated with or without 1 μM tZ for 1 h. Luciferase activity was normalized to *35S:rLUC* and is indicated as relative values, with that for the effector control (empty vector) set to 1. Data are presented as mean ± SD (n = 3). Significant differences from the non-treated control were determined by Student's *t*-test: **, $P < 0.01$.

(D and E) GUS staining of roots of 5-day-old wild-type, *arr1-3* (D) and *arr12-1* (E) harboring the *ProCCS52A1:GUS* reporter gene. Bars = 100 μm.

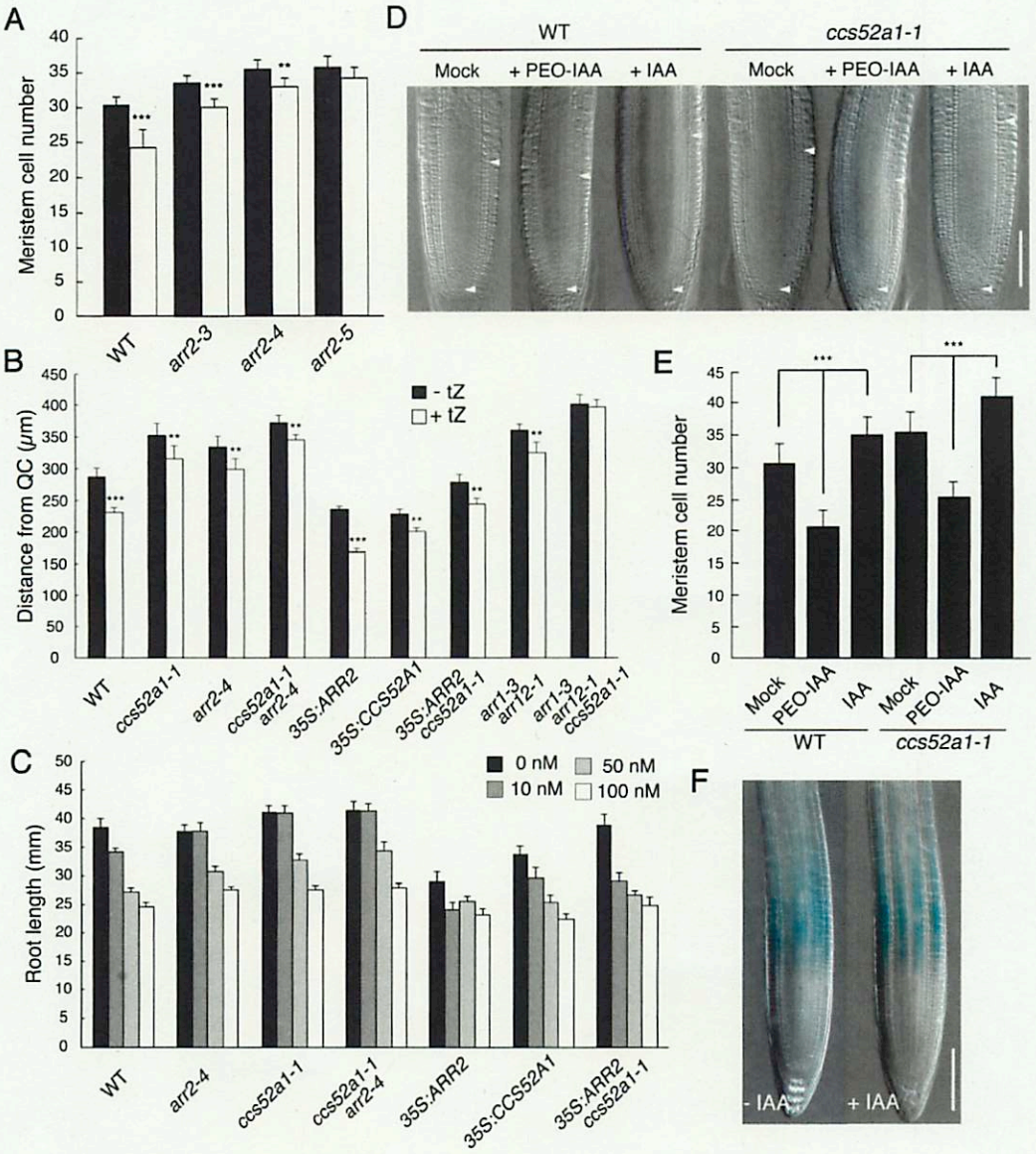

Figure S3 (Related to Figure 3). ARR1/12-, ARR2- and CCS52A1-mediated control of endocycle onset and root meristem size.

(A) Cortex cell number in the meristematic zone. Five-day-old seedlings were treated with or without 1 μM tZ for 16 h, and cell number was counted. Data are presented as mean ± SD (n > 30). Significant differences from the non-treated control were determined by Student's *t*-test: **, $P < 0.01$; ***, $P < 0.001$.

(B) Distance from the QC to the first endoreduplicated cell, as estimated by an increase of > 1.5-fold in nuclear area. Five-day-old seedlings were treated with or without 1 μM tZ for 16 h, and nuclei of roots were stained with DAPI. Data are presented as mean ± SD (n > 15). Significant differences from the non-treated control were determined by Student's *t*-test: **, $P < 0.01$; ***, $P < 0.001$.

(C) Root length of 10-day-old seedlings. Plants were grown on media containing 0, 10, 50, or 100 nM tZ. Data are presented as mean ± SD (n > 25).

(D) Root meristem size in 5-day-old wild-type and *ccs52a1-1* seedlings. Plants were treated with 10 μM PEO-IAA or 0.5 nM IAA for 24 h, or mock-treated. Arrowheads indicate the QC and the first elongated cell in the cortex cell file. Bar = 100 μm.
(E) Cortex cell numbers in the meristematic zones shown in (D). Data are presented as mean ± SD (n > 20). Significant differences were determined by Student's *t*-test: ***, $P < 0.001$.
(F) GUS staining of 5-day-old roots harboring the *ProCCS52A1:GUS* reporter gene. Plants were untreated (-IAA) or treated (+IAA) with 0.5 nM IAA for 1 h. Bar = 100 μm.

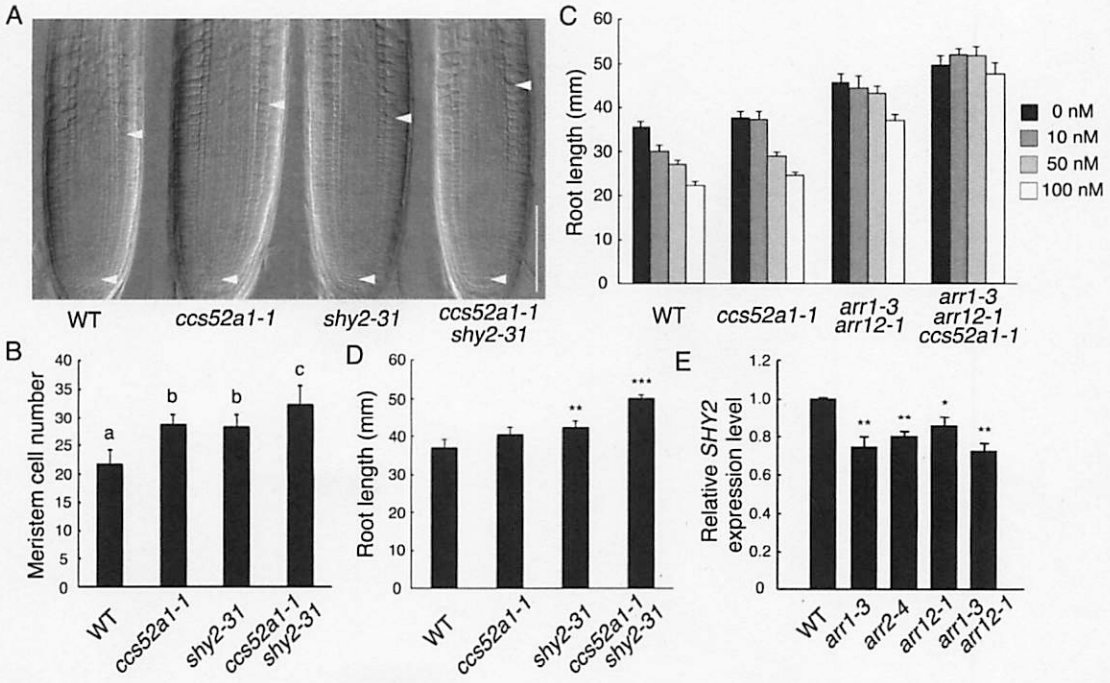

Figure S4 (Related to Figure 4). Genetic interaction between *CCS52A1*, *ARR1/12* and *SHY2*, and *SHY2* expression in *arr* mutants.

(A) Root meristem of 5-day-old wild-type, *ccs52a1-1*, *shy2-31*, and *ccs52a1-1 shy2-31* seedlings. Arrowheads indicate the QC and the first elongated cell in the cortex cell file. Bar = 100 μm.

(B) Cortex cell numbers in the meristematic zones shown in (A). Data are presented as mean ± SD (n > 35). Significant differences were determined by Student's *t*-test. Bars with different letters differ significantly from each other ($P < 0.05$).

(C) Root length of 10-day-old seedlings. Plants were grown on media containing 0, 10, 50, or 100 nM tZ. Data are presented as mean ± SD (n > 25).

(D) Root length of 10-day-old seedlings. Data are presented as mean ± SD (n > 25). Significant differences from the wild-type were determined by Student's *t*-test: **, $P < 0.01$; ***, $P < 0.001$.

(E) ARR2 controls *SHY2* expression. Total RNA from 5-day-old roots was subjected to real-time qRT-PCR. The expression levels of *SHY2* were normalized to that of *TUBULIN4*, and are indicated as relative values, with that for wild-type set to 1. Data are presented as mean ± SD (n = 3). Significant differences from the wild-type were determined by Student's *t*-test: *, $P < 0.05$; **, $P < 0.01$.

Table S1. Primers Used for Cloning and ChIP Assay

Yeast one-hybrid assay	
ARR1	5'-AAAAAGCAGGCTTCATGATGAATCCGAGTCACGGAAG-3'
	5'-AGAAAGCTGGGTCTCAAACCGGAATGTTATCGATG-3'
ARR1ΔDDK	5'-AAAAAGCAGGCTTCGTTAGGAAGAGGAGAAGTGAATG-3'
	5'-AGAAAGCTGGGTCTCAAACCGGAATGTTATCGATG-3'
ARR2	5'-AAAAAGCAGGCTTCATGGTAAATCCGGGTCACGGAAG-3'
	5'-AGAAAGCTGGGTCTCAGACCTGGATATTATCGATG-3'
ARR2ΔDDK	5'-AAAAAGCAGGCTTCTCTGAACATTCTGGAGGAAGTATTG-3'
	5'-AGAAAGCTGGGTCTCAGACCTGGATATTATCGATG-3'
ARR10	5'-AAAAAGCAGGCTTCATGACTATGGAGCAAGAAATTG-3'
	5'-AGAAAGCTGGGTCTCAAGCTGACAAAGAAAAGGGA-3'
ARR10ΔDDK	5'-AAAAAGCAGGCTTCCTTAAGAAGAATAAGAGCAATG-3'
	5'-AGAAAGCTGGGTCTCAAGCTGACAAAGAAAAGGGA-3'
ARR12	5'-AAAAAGCAGGCTTCATGACTGTTGAACAAAATTTAG-3'
	5'-AGAAAGCTGGGTCTCATATGCATGTTCTGAGTGAAC-3'
ARR12ΔDDK	5'-AAAAAGCAGGCTTCTTTGATAAGAACCGTGGGAGTA-3'
	5'-AGAAAGCTGGGTCTCATATGCATGTTCTGAGTGAAC-3'
Protoplast transactivation assay	
ARR1	5'-AAAAAGCAGGCTTCATGATGAATCCGAGTCACGGAAG-3'
	5'-AGAAAGCTGGGTCTCAAACCGGAATGTTATCGATG-3'
ARR1ΔDDK	5'-AAAAAGCAGGCTTCATGGTTAGGAAGAGGAGAAGTGAATG-3'
	5'-AGAAAGCTGGGTCTCAAACCGGAATGTTATCGATG-3'
ARR2	5'-AAAAAGCAGGCTTCATGGTAAATCCGGGTCACGGAAG-3'
	5'-AGAAAGCTGGGTCTCAGACCTGGATATTATCGATG-3'
ARR2ΔDDK	5'-AAAAAGCAGGCTTCATGTCTGAACATTCTGGAGGAAGTATTG-3'
	5'-AGAAAGCTGGGTCTCAGACCTGGATATTATCGATG-3'
ARR10	5'-AAAAAGCAGGCTTCATGACTATGGAGCAAGAAATTG-3'
	5'-AGAAAGCTGGGTCTCAAGCTGACAAAGAAAAGGGA-3'
ARR10ΔDDK	5'-AAAAAGCAGGCTTCATGCTTAAGAAGAATAAGAGCAATG-3'
	5'-AGAAAGCTGGGTCTCAAGCTGACAAAGAAAAGGGA-3'
ARR12	5'-AAAAAGCAGGCTTCATGACTGTTGAACAAAATTTAG-3'
	5'-AGAAAGCTGGGTCTCATATGCATGTTCTGAGTGAAC-3'
ARR12ΔDDK	5'-AAAAAGCAGGCTTCATGTTTGATAAGAACCGTGGGAGTA-3'

	5'-AGAAAGCTGGGTCTCATATGCATGTTCTGAGTGAAC-3'
ChIP assay	
Fragment #1	5'-TTGGTTAAACGGCTATAATCGTTAG-3'
	5'-CAGTATGAAAGTTGGGGGGACTCTCTG-3'
Fragment #2	5'-TTTGATTTATTAATCTCTTTTTCCAAC-3'
	5'-TAGCTTACTGGAGAAGATGCTTG-3'
Fragment #3	5'-CAACTTGCAATCAATTTTTACTC-3'
	5'-ATAATCCAATCAAATATAACAAAAGAC-3'
Fragment #4	5'-TGGTTTATACTTTGTATCTCAATTCTG-3'
	5'-TATACTAGTCAAAAATGGTTCAATG-3'
Fragment #5	5'-TCTGTACTTTTGTGTCTCACAATTCTC-3'
	5'-CAAATCAAGCCAAAACATGC-3'
Fragment #6	5'-CTGCCATCTAAGATTCTTCTAC-3'
	5'-GAGGACCGTGAGGTTTAAGC-3'
Fragment #7	5'-TTTCTGTTTTTCCTTAGATTTCC-3'
	5'-TTTGTTGAAGTGTTGTTGAAACATC-3'
CCS52A1 promoter dissection	
-1490 to -1	5'-GGTCGACTTATCATTTGTTTTCTGATTTTTCTTCT-3'
	5'-GGGATCCATTGGTTTTTTTTTTTTGTTGACTC-3'
-1190 to -1	5'-GGTCGACTTTGATTTATTAATCTCTTTTTC-3'
	5'-GGGATCCATTGGTTTTTTTTTTTTGTTGACTC-3'
-1090 to -1	5'-GGTCGACATTTTCCACCTACACATCAA-3'
	5'-GGGATCCATTGGTTTTTTTTTTTTGTTGACTC-3'
-990 to -1	5'-GGTCGACTCAATTTTTACTCATTTTAGTAA-3'
	5'-GGGATCCATTGGTTTTTTTTTTTTGTTGACTC-3'
-890 to -1	5'-GGTCGACATCAATTTCTTATAGTTGACAGAAAAAA-3'
	5'-GGGATCCATTGGTTTTTTTTTTTTGTTGACTC-3'
-790 to -1	5'-GGTCGACTTATATCTTTGATATTTAAGTTT-3'
	5'-GGGATCCATTGGTTTTTTTTTTTTGTTGACTC-3'
-690 to -1	5'-GGTCGACTATTAAGAAAATTAAAATTAATTTCTTA-3'
	5'-GGGATCCATTGGTTTTTTTTTTTTGTTGACTC-3'

Supplemental Experimental Procedures

Plant growth conditions

Arabidopsis thaliana (ecotype Col-0) was grown vertically on Murashige and Skoog (MS) plates [0.5 x MS salts, 0.5 g/l 2-(*N*-morpholino)ethanesulfonic acid (MES), 1% sucrose, and 0.8% gellan gum (pH 5.7)] under long-day conditions (16 h light/8 h dark cycle) at 22 °C.

Plant materials

ccs52a1-1, *35S:CCS52A1* [1], *arr2-4* [2], *arr1-3*, *arr12-1*, *arr1-3 arr12-1* [3], *ahk3-1*, *ahk4-1*, *ahk3-1 ahk4-1* [4], *ip3-2 ipt5-1 ipt7-1* [5], *35S:CKX2* [6], *35S:ARR2*, *35S:ARR2-HA* [7], *ProCCS52A1:GUS*, *ProCCS52A1:NLS-GFP* [8] and *ProARR2:ARR2:GUS* [9] were described previously. *shy2-31* (L*er* background) [10] was backcrossed to Col-0 wild-type twice and used for analysis.

GUS staining

After samples were washed in phosphate buffer, they were incubated in GUS staining solution [100 mM sodium phosphate, 1 mg/ml 5-bromo-4-chloro-3-indolyl ß-D-glucuronide, 0.5 mM ferricyanide and 0.5 mM ferrocyanide (pH 7.4)] in the dark at 37 °C. The samples were then cleared in a mixture of chloral hydrate, glycerol and water (8 g:1 ml:1 ml).

Microscopy

For visualization of nuclei in roots, 5-day-old seedlings were fixed in a mixture of ethanol, formaldehyde and acetic acid (17:2:1), and stained with 4',6-diamidino-2-phenylindole (DAPI). Nuclear size and distance from the QC were measured for individual cortex cells

with ImageJ software (NIH). The root meristem was observed with samples either cleared in a mixture of chloral hydrate, glycerol and water, or stained with propidium iodide (PI) as described by Adachi et al. [11].

Chromatin immunoprecipitation

A ChIP experiment was performed as described previously [12] with minor modifications. Using 2-week-old *35S:ARR2-HA* seedlings, chromatin bound to ARR2 proteins was precipitated with anti-hemagglutinin (HA) antibodies (Abcam). Col-0 seedlings were used as a negative control. To quantify the precipitated chromatin, specific primer sets that cover the *CCS52A1* promoter from the transcription start site to -1500 bp, with 150-bp intervals, were used for real-time qPCR.

Yeast one-hybrid assay

The *CCS52A1* promoter was PCR-amplified using the primers 5'-ATGGCGGCCGCTTATCATTTGTTTTCTGATT-3' and 5'-ATGGCGGCCGCTGGTTTTTTTTTTTTGTTGACT-3', and cloned into the pINT1-HIS3NB vector [13] to generate a transcriptional fusion with the *HIS3* gene. The coding regions of *ARR1*, *ARR1ΔDDK*, *ARR2* and *ARR2ΔDDK* were PCR-amplified using the primers shown in Table S1, and cloned into pGADT7 (Clontech) to generate a translational fusion with the GAL4 activation domain. Plasmids were introduced into yeast strain AH109 (Clontech) according to the Yeast Protocol Handbook (Clontech). For the one-hybrid assay, transformants were spotted on a plate with or without histidine in the presence of 5 mM 3-amino-1,2,4-triazole (3-AT).

Protoplast transactivation assay

To make the reporter construct, the 1.5-kb *CCS52A1* promoter was PCR-amplified using the primers 5'-ATGCCTGCAGTTATCATTTGTTTTCTGATT-3' and 5'-CATGGTCGACACATTGCTTGCTGTAGGATCTTC-3', and cloned into the 35S-GAL4UAS-LUC vector [14] to generate a transcriptional fusion with the firefly luciferase (fLUC) gene. To make effector constructs, the coding regions of GFP (negative control), *ARR1*, *ARR1ΔDDK*, *ARR2*, *ARR2ΔDDK*, *ARR10*, *ARR10ΔDDK*, *ARR12* and *ARR12ΔDDK* were PCR-amplified using the primers shown in Table S1, and cloned into p35SG [32] to generate a transcriptional fusion with the cauliflower mosaic virus 35S promoter. Protoplasts prepared from an *Arabidopsis* Deep cell culture were cotransfected with the reporter plasmid, effector plasmids, and a normalization construct carrying the rLUC gene under the 35S promoter. After transfection, protoplasts were incubated at 22 °C for 16 h, and fLUC and rLUC activities were measured with the Dual-Luciferase reporter system (Promega) using a Mithras LB940 microplate reader (Berthold).

Ploidy measurement

To measure the C-value of nuclei in roots, 5-day-old seedlings were fixed in 4% paraformaldehyde in PBS for 50 min at 25 °C. They were stained with a mixture of DAPI staining solution (CyStainUV Precise P, PARTEC) and PBS (1:4) for 4 min, washed three times with PBS and mounted in 30% 2,2'-thiodiethanol. The slides were placed on the inverted platform of a FluoView FV1000 confocal microscopic system (Olympus, Tokyo, Japan). Images were acquired with a 40 × objective lens. Image processing and C-value

analyses were performed with MetaMorph microscopy automation and image analysis software (Molecular Devices, CA, USA).

Promoter deletion analysis

Genomic fragments encompassing different regions of the *CCS52A1* promoter were PCR-amplified from *Arabidopsis* genomic DNA using the primers listed in Table S1. Each PCR fragment was cloned into pBI101 (Clontech) to generate a transcriptional fusion with the GUS gene. These constructs were introduced into *Arabidopsis* plants by the floral dip method [15], and transgenic lines were selected on kanamycin-containing medium. Promoter activity was observed by GUS staining.

Quantitative RT-PCR

Total RNA was extracted from *Arabidopsis* roots with an RNeasy Plant Mini Kit (QIAGEN). First-strand cDNAs were prepared from total RNA with the Superscript II First-Strand Synthesis System (Invitrogen) according to the manufacturer's instructions. Quantitative PCR was performed with a THUNDERBIRD SYBR qPCR Mix (Toyobo) with 100 nM primers and 0.1 μg of first-strand cDNAs. The following primers were used: 5'-AGAGGTTGACGAGCAGATGA-3' and 5'-CCTCTTCTTCCTCCTCGTAC-3' for *TUBULIN4*, 5'-CTGGATCGGTGGTTCCATTC-3' and 5'-CCTGGACCTGCCTCATCATAC-3' for *ACTIN2*, 5'-GAAACATCCCCTCCTCGAAAGGCTC-3' and 5'-AAGCTTTAAGCAACTCTGAGTATCC-3' for *SHY2*, and 5'-CACGCTGCAAGAGAACAAGA-3' and 5'-ACCACTTGAGTCCGCATACC-3' for

CCS52A1. PCR reactions were conducted with the LightCycler 480 Real-Time PCR System (Roche) according to the following conditions: 95 °C for 5 min; 45 cycles at 95 °C for 10 sec, at 60 °C for 10 sec, and at 72 °C for 15 sec.

Supplemental References

1. Larson-Rabin, Z., Li, Z., Masson, P.H., and Day, C.D. (2009). *FZR2/CCS52A1* expression is a determinant of endoreduplication and cell expansion in Arabidopsis. Plant Physiol. *149*, 874-884.
2. Kim, K., Ryu, H., Cho, Y.H., Scacchi, E., Sabatini, S., and Hwang, I. (2012). Cytokinin-facilitated proteolysis of ARABIDOPSIS RESPONSE REGULATOR 2 attenuates signaling output in two-component circuitry. Plant J. *69*, 934-945.
3. Mason, M.G., Mathews, D.E., Argyros, D.A., Maxwell, B.B., Kieber, J.J., Alonso, J.M., Ecker, J.R., and Schaller, G.E. (2005). Multiple type-B response regulators mediate cytokinin signal transduction in *Arabidopsis*. Plant Cell *17*, 3007-3018.
4. Nishimura, C., Ohashi, Y., Sato, S., Kato, T., Tabata, S., and Ueguchi, C. (2004). Histidine kinase homologs that act as cytokinin receptors possess overlapping functions in the regulation of shoot and root growth in Arabidopsis. Plant Cell *16*, 1365-1377.
5. Miyawaki, K., Tarkowski, P., Matsumoto-Kitano, M., Kato, T., Sato, S., Tarkowska, D., Tabata, S., Sandberg, G., and Kakimoto, T. (2006). Roles of Arabidopsis ATP/ADP isopentenyltransferases and tRNA isopentenyltransferases in cytokinin biosynthesis. Proc. Natl. Acad. Sci. USA *103*, 16598-16603.
6. Werner, T., Motyka, V., Laucou, V., Smets, R., Van Onckelen, H., and Schmülling, T. (2003). Cytokinin-deficient transgenic Arabidopsis plants show multiple developmental

alterations indicating opposite functions of cytokinins in the regulation of shoot and root meristem activity. Plant Cell *15*, 2532-2550.

7. Choi, J., Huh, S.U., Kojima, M., Sakakibara, H., Paek, K.H., and Hwang, I. (2010). The cytokinin-activated transcription factor ARR2 promotes plant immunity via TGA3/NPR1-dependent salicylic acid signaling in *Arabidopsis*. Dev. Cell *19*, 284-295.
8. Vanstraelen, M., Baloban, M., Da Ines, O., Cultrone, A., Lammens, T., Boudolf, V., Brown, S.C., De Veylder, L., Mergaert, P., and Kondorosi, E. (2009). APC/C^{CCS52A} complexes control meristem maintenance in the *Arabidopsis* root. Proc. Natl. Acad. Sci. USA *106*, 11806-11811.
9. Mason, M.G., Li, J., Mathews, D.E., Kieber, J.J., and Schaller, G.E. (2004). Type-B response regulators display overlapping expression patterns in Arabidopsis. Plant Physiol. *135*, 927-937.
10. Knox, K., Grierson, C.S., and Leyser, O. (2003). AXR3 and SHY2 interact to regulate root hair development. Development *130*, 5769-5777.
11. Adachi, S., Minamisawa, K., Okushima, Y., Inagaki, S., Yoshiyama, K., Kondou, Y., Kaminuma, E., Kawashima, M., Toyoda, T., Matsui, M., et al. (2011). Programmed induction of endoreduplication by DNA double-strand breaks in *Arabidopsis*. Proc. Natl. Acad. Sci. USA *108*, 10004-10009.
12. Saleh, A., Alvarez-Venegas, R., and Avramova, Z. (2008). An efficient chromatin immunoprecipitation (ChIP) protocol for studying histone modifications in *Arabidopsis* plants. Nat. Protoc. *3*, 1018-1025.
13. Lopato, S., Bazanova, N., Morran, S., Milligan, A.S., Shirley, N., and Langridge, P. (2006). Isolation of plant transcription factors using a modified yeast one-hybrid system.

Plant Methods *2*, 3.

14. Yamaguchi, M., Ohtani, M., Mitsuda, N., Kubo, M., Ohme-Takagi, M., Fukuda, H., and Demura, T. (2010). VND-INTERACTING2, a NAC domain transcription factor, negatively regulates xylem vessel formation in *Arabidopsis*. Plant Cell *22*, 1249-1263.
15. Clough, S.J., and Bent, A.F. (1998). Floral dip: a simplified method for *Agrobacterium*-mediated transformation of *Arabidopsis thaliana*. Plant J. *16*, 735-743.